COMPARATIVE STUDY ON BREAKING WAVE FORCES ON VERTICAL WALLS WITH CANTILEVER SURFACES

Kisacik[1] Dogan; Van Bogaert[1], Philippe; Troch[1], Peter
Department of Civil Engineering, Ghent University,
Technologiepark 904, Ghent, 9052, Belgium

ABSTRACT

Physical experiments (at a scale of 1/20) are carried out using two different models: a vertical wall with cantilevering slab and a simple vertical wall. Tests are conducted for a range of values of water depth, wave period and wave height. The largest peak pressures were recorded at the SWL ($82 * \rho g h_s$) on the vertical part and at the fixed corner of the cantilever slab ($90 * \rho g h_s$). Pressure measurements and derived force calculations on the simple vertical wall were used to evaluate the existing prediction formulas. A significant effect of the cantilevering part is observed on the total horizontal force and overturning moment of a simple vertical wall. This is due to secondary impact occurring on the overhanging part by a jet climbing on the vertical part.

KEY WORDS: Wave impact pressure; wave impact force; small scale tests, regular waves; wave breaking.

INTRODUCTION

Vertical breakwaters and seawalls are frequently used to protect land from sea action such as high water levels and waves. To reduce the overtopping, coastal engineers provide the vertical walls with a return crown wall or even a horizontal cantilever slab. However, wave impacts on the horizontal structure introduce an important uplifting force. The lift forces consist of impact loads which one of high magnitude and short duration. It is reasonably impossible to substitute these impact effects by a static equivalent. A detailed description of the space and time distribution of the wave impacts thus becomes imperative. The Pier of Blankenberge which is located along the Belgian coast is an illustrative example of a vertical wall with cantilever surfaces (Verhaeghe et al., 2006).

The qualitative and quantitative determination of wave loads on vertical walls has already been examined intensively in the past decades (e.g. Oumeraci et al., 2001; Allsop et al, 1996; Goda, 2000; Cuomo et al., 2009). Uplift loads below horizontal cantilever surfaces are frequently examined in various research projects (McConnell et al., 2003; Cuomo et al., 2007). In opposition to a single vertical or horizontal wall, structures consisting of both vertical parapets and horizontal cantilever slabs have scarcely been considered. A consensus on the necessary approach for the research of this type of structures lacks completely (Okamura, 1993). Due to the special geometry, involving closed angles, which do not allow incident waves to dissipate, the wave kinematics differ fundamentally from the preceding situations.

In this sense, the main objective of the present research is to bring a new design tool to assess violent water wave impacts on a vertical wall, including an overhanging horizontal cantilever slab, based on the correlation between the kinematics of breaking waves. In this particular research, model tests with a scale of 1/20 were carried out to fulfill the above goals and results are compared with the test data of simple vertical case in identical conditions.

Within this paper, an overview of the small scale model tests set up will be provided. This will be followed by the comparison of measured horizontal forces and overturning moments with the results of a simple vertical wall and well known theoretical values in the literature (Minikin, 1963; Goda, 2000; Blackmore & Hewson, 1984; Allsop et al., 1996; Oumeraci et al., 2001; Cuomo et al., 2007). Based on the discussion of the test results, conclusions will be formulated.

LITERATURE REVIEW

Waves attacking vertical structures are usually classified as non breaking, breaking and broken waves. Breaking waves create short impulsive loads on the vertical structures which introduce localized damages. Coastal structures are bulk structures and most researchers did not consider these short-duration loads in their design formulas. However, Oumeraci (1994) emphasise the importance of impulsive loads in the design of vertical structures. Several formulas from design codes allow calculating impulsive loads on vertical structures.

Minikin (1963) suggests a parabolic pressure distribution for the breaking waves on vertical walls. The dynamic pressure p_m (Eq. 1) has a maximum value at the SWL and decreases to zero at $0.5H_b$ below and above the SWL. The total horizontal force represented by the area under the dynamic and hydrostatic pressure distribution is shown in Eq. 2 (SPM, 1984).

$$p_m = 101\rho g \frac{H_b}{L_D}\frac{h_s}{D}(D + h_s) \quad (1)$$

$$F_h = \frac{101}{3}\rho g \frac{H_b^2}{L_D}\frac{h_s}{D}(D + h_s) + 0.5\rho g H_b h_s\left(1 + \frac{H_b}{4}\right) \quad (2)$$

Where D is the depth at one wavelength in front of the wall, L_D is the wavelength in water depth D and H_b is the breaker wave height.

Minikin formula is dimensionally inconsistent. Allsop et al. (1996c) show that the horizontal impact force (F_h) predicted by Minikin's formula is incorrect due to the decrease of F_h with increasing L_D. There are some incompatibilities are found between different versions of the Minikin's formula which are mainly due to a unit mistake converting from British to metric units. Therefore, Minikin's formula is out of fashion in recent years (Bullock, et al., 2004).

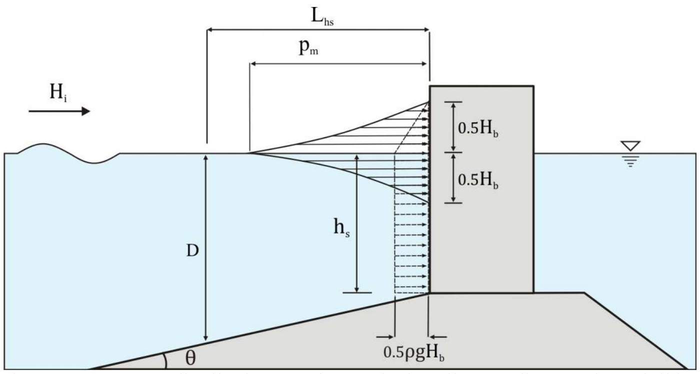

Figure 1. Pressure distribution on the vertical wall according to the Minikin Method.

Goda (1974) suggests his own formula for the wave loads on the vertical walls based on theoretical and laboratory works. He assumes a trapezoidal pressure distribution on the vertical walls with maximum pressure at the SWL (Eq.3). His method predicts a static equivalent load instead of short impulsive loads for breaking and non breaking waves. Takahashi (1996) extends the Goda method for breaking waves by adding some new term in the maximum pressure (p_1) at SWL to take into account the effect of berm dimension.

$$p_1 = 0.5(1 + \cos\beta)(\lambda_1\alpha_1 + \lambda_2\alpha_* \cos^2\beta)\rho g H_{max} \quad (3)$$

Where β is the angle of incidence of the wave attack with respect to a line perpendicular to the structure, $\lambda_1, and\ \lambda_2$ are the multiplication factors depending on the geometry of the structure. For conventional vertical wall structures, $\lambda_1 = \lambda_2 = 1$ and H_{max} is the highest wave out of the surf zone or is the highest of random breaking waves at a distance of $5H_s$ seaward of the structure. The total horizontal force is calculated from the area under the pressure profile shown in Fig. 2.

Blackmore & Hewson (1984) suggest a prediction formula based on full-scale field measurements (Eq. 4). They consider the effect of entrained air which results in a reduction in the impact pressure of field tests compared to laboratory tests.

$$p_1 = \lambda\rho C_b^2 T \quad (4)$$

Where C_b is the shallow water wave celerity and λ is the aeration factor with dimension [s^{-1}]. λ has a value between $0.1s^{-1}$ and $0.5s^{-1}$ at full scale and between $1s^{-1}$ and $10s^{-1}$ at model scale (Blackmore & Hewson, 1984). It is recommended to use value of $0.3s^{-1}$ for rocky foreshore and $0.5s^{-1}$ for regular beaches (BS 6349). The total horizontal force is calculated from the area under the pressure profile shown in Fig. 3.

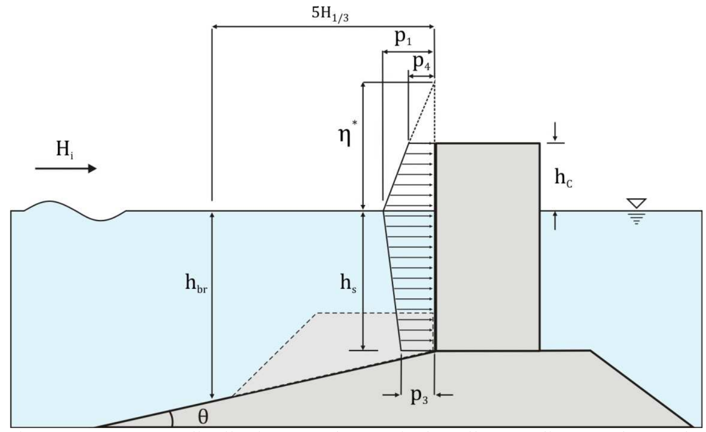

Figure 2. Pressure distribution on the vertical wall according to the Goda Method.

According to the model tests at HR Wallingford within the PROVERBS project, Allsop & Vicinanza (1996) recommend a prediction formula for horizontal wave impact force on the vertical walls (Eq.5). Data were produced on a slope of 1/50 at 1/250 level for the range of 0.3<Hs/d≤2. The method is recommended in Oumeraci et al. (2001) for preliminary design.

$$F_h = 15\rho g h_s^2 (H_{si}/h_s)^{3.134} \quad (5)$$

Where h_s and H_{si} are the water depth and significant wave height at the model toe.

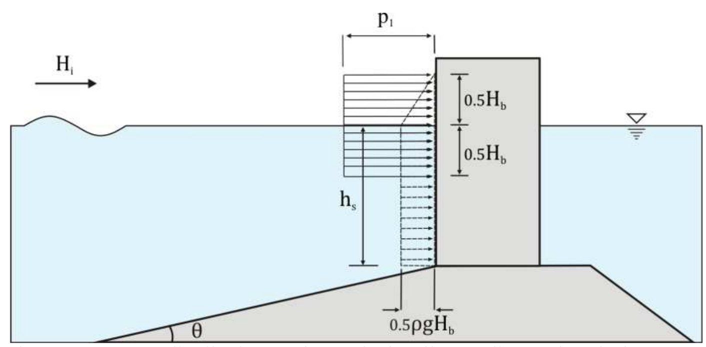

Figure 3. Pressure distribution on the vertical wall according to the Blackmore & Hewson Method.

PROVERBS was an EU project to develop and implement probability based tools for an integrated design of vertical breakwaters. Within PROVERBS a prediction method has been developed based on large data sets include small and large scale physical tests and field measurements. The overall horizontal impact force on the vertical breakwater is calculated from Eq. 6.

$$F_h^* = F_h/\rho g H_b^2 \quad (6)$$

Where H_b is the breaking wave height and F_h^* is the relative maximum wave force calculated using this generalized extreme value (GEV) distribution (Eq.7).

$$F_h^* = \frac{\alpha}{\gamma}\{1 - [-lnP(F_h^*)]^\gamma\} + \beta \quad (7)$$

Where $P(F_h^*)$ is the probability of non exceedance of the impact force (generally taken as 90%) and α, β, γ are the statistical parameters for GEV distribution and changing with bed slope. The pressure profile on the vertical walls according to PROVERBS is shown in Fig. 4.

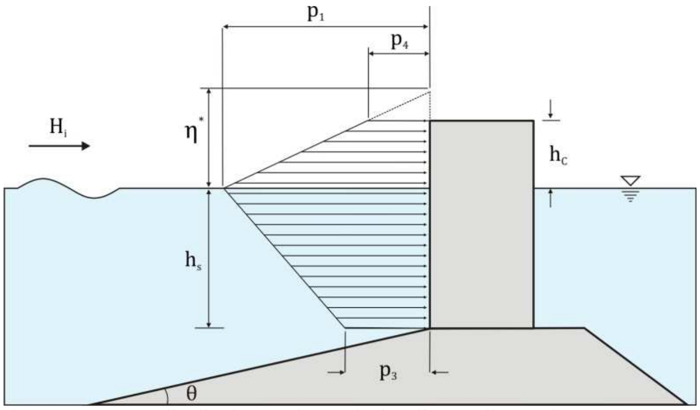

Figure 4. Pressure distribution on the vertical wall according to the PROVERBS.

Cuomo et al, (2010) recently suggest a prediction formula for the horizontal impulsive load $F_{h,imp,1/250}$ on the vertical walls on level of 1/250 (Eq. 8).

$$F_{h,imp,1/250} = \rho g \cdot H_{mo} \cdot L_{hs} \cdot \left(1 - \frac{|h_b - h_s|}{h_s}\right) \tag{8}$$

Where L_{hs} is the wavelength at the toe of the structure for $T = T_m$, h_s is the water depth at the structure and h_b is the water depth at breaking. h_b is determined from Miche's breaking criteria (Eq. 9) by assuming $H_b = H_{mo}$

$$h_b = \frac{1}{k} arctanh\left(\frac{H_{mo}}{0.14 \cdot L_{hs}}\right) \tag{9}$$

Where k is calculated from, $k = 2\pi / L_{hs}$

Eq. 8 is valid in the range of $0.2\ m < H_{mo} < 0.7\ m$, $0.5\ m < h_s < 1.3\ m$ and $2\ s < T_m < 3.7\ s$.

EXPERIMENTAL SET-UP

Physical model tests are carried out in the wave flume (30 m x 1 m x 1.2 m) of Ghent University, Belgium. The model is located 22.5 m away from the wave paddle on a uniform slope with 50 cm depth at the location of the structure. The model is 30 cm high and 60 cm long (Model-A). A second model which is a simple vertical wall (Model-B) is also tested in the same conditions allow comparing the results and assess the effect of the overhanging part. The foreshore slope is 1/20 (see Fig. 5).

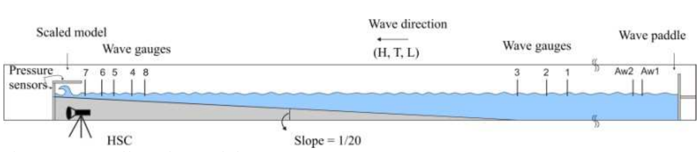

Figure 5. Small-scale model set up.

Models are instrumented with pressure sensors to register wave impact pressures and related forces both on the vertical and horizontal parts. The accuracy of the pressure profiles mainly depends on the spatial resolution of the pressure sensors, since 10 sets of pressure sensors are used to achieve the goals. These are quartz pressure sensors developed for measuring dynamic and quasi-static pressures up to 2 bar. Diameters of the sensors are 6 mm and they have a high natural frequency around 150 kHz. The required supplementary items for measuring the pressures are signal conditioners with a maximum of 20 kHz sampling frequency and mounting adaptors for fixation of sensors on the model.

Both models (Model-A & Model-B) are tested under the same wave conditions. Tests are carried out for 18 regular waves and each test is repeated without model to measure the undisturbed wave height at the location of structures. In addition, wave heights are measured at various locations like 5Hs before the structure. In the model tests, the wave period T, wave height H and water depth (h_s) are considered as variable input parameters. Tests are conducted for four different values of water depth and wave period. For each combination of parameters, wave heights ranging from non breaking to broken waves are considered and measurements are done for a wave train of 18 regular waves. The matrix of parameters is summarized in Table 1.

Table 1. Test parameter matrix

Water depth at the structure h_s (m)	Wave period T (s)	Wave height H range
0.075	2.2, 2.4, 2.6, 2.8	from non breaking to broken waves
0.105	2.2, 2.4, 2.6, 2.8	from non breaking to broken waves
0.135	2.2	from non breaking to broken waves
0.165	2.2	from non breaking to broken waves

Within the scope of this paper, in particular results of h_s=0.135 m, T=2.2 s and wave heights breaking at the structure are considered.

The total horizontal force and related overturning moment acting on the model is calculated by integrating the pressure results on the vertical part (Eq. 10).

$$F_h(t) = \sum_{k=1}^{n-1} (p_k(t) + p_{k+1}(t))/2 * \Delta z_k \tag{10}$$

Where $p_k(t)$ is the measured instantaneous pressure at the location of the k-th sensor, Δz_k is the distance between two sensors and n is the number of sensors on the vertical part. The related overturning moment is given in Eq. 11.

$$M(t) = \sum_{k=1}^{n-1} (p_k(t) + p_{k+1}(t))/2 * \Delta z_k * \Delta z'_k \tag{11}$$

Where $\Delta z'_k$ is the moment lever.

As an example, the horizontal force $F_h(t)$ time series at the SWL (h_s=0.135 m) is shown in Fig. 6 during a time interval which shows several associated impacts, for regular waves with wave period T=2.2 s, and sampling frequency 20 kHz. As it is well known from literature, the variations in the peak pressure values are high and not repeatable.

Fig. 7 and Fig. 8 show the spatial distribution of the local peak pressure values on the vertical and horizontal parts respectively on a time interval from thirty individual impacts of regular waves with target wave height Hi= 0.115m, wave period T=2.2s and sampling frequency 20 kHz. The largest peak pressures were recorded at the SWL ($82 * \rho g h_s$) on the vertical part and at the corner of the horizontal part ($90 * \rho g h_s$). Pressures on the vertical wall are increased by the effects appearing in the upper corner where the wall is fixed to the cantilever surfaces.

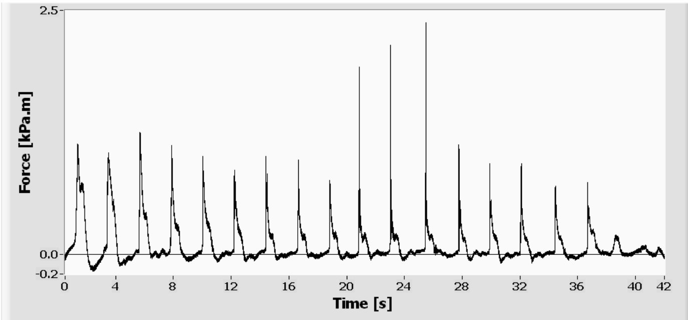

Figure 6. Time series of the horizontal force $F_h(t)$ record for the simple vertical model (h_s=0.135 m, Hi=0.115 m and T=2.2 s).

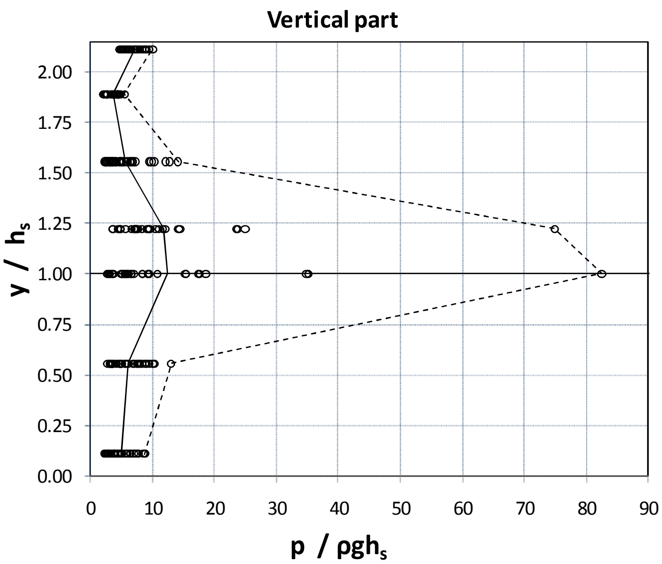

Figure 7. Local peak pressure distribution on the vertical part of Model-A for thirty regular waves (h_s=0.135m, T=2.2s, sampling frequency=20 kHz and Hi=0.115m). Dashed and solid lines indicate maximum and mean peak pressure values respectively

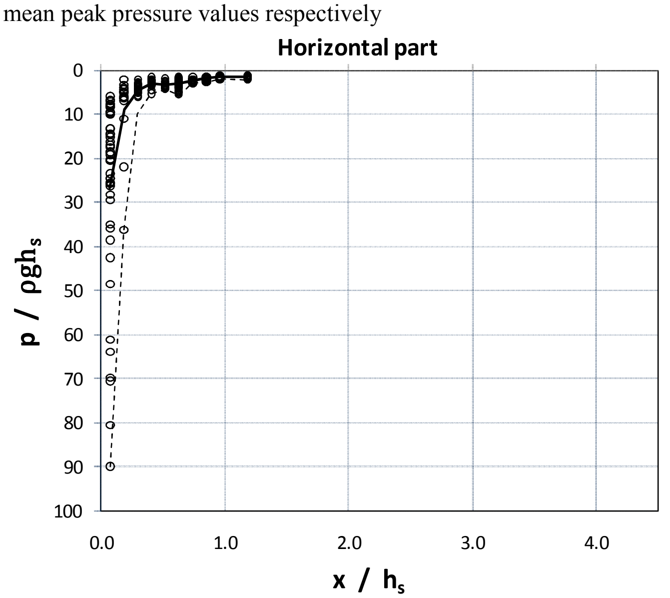

Figure 8. Local peak pressure distribution on the horizontal part of Model-A for thirty regular waves (h_s=0.135m, T=2.2s, sampling frequency=20 kHz and Hi=0.115m). Dashed and solid lines indicate maximum and mean peak pressure values respectively

COMPARISION WITH EXISTING PREDICTION METHODS

Fig. 9~14 shows the comparison of measured horizontal forces F_h on a vertical wall (Model-B) with the existing well known prediction formulas for various values of the wave height (H). Force F_h and H are normalized by $\rho g h_s$ and water depth (h_s) respectively. All these methods are developed for irregular waves and considered statistical wave height values like Hs or Hmax to calculate the force. In this particular set of data, force and wave height, measured by zero down crossing method, are correlated directly rather than showing a statistical relation. The data set contains results of breaking waves within the range of waves 0.6<H/h_s<1.1. These are breaking waves changing from breaking with small air trapping to well developed breaking with large air trapping. The measured data are showing high scatter.

Both Minikin and extended Goda methods are under predicting the horizontal forces on the vertical walls. In all methods, Hb is considered as the height of incident waves (Hi) at the location of structure (h_s) however the Goda method is considered incident wave heights 5H before the structure. The Allsop & Vicinanza formula is under predicting some of the values but shows a good agreement with the trend of data. Results from the Blackmore & Hewson method shows an envelope line for the measurements with an aeration factor 10 which is the highest value suggested for small scale tests. Proverb methods mainly over estimates the force except for the waves creating very high impact around H/h_s=1 and the Cuomo method shows good agreement with our data except for few points in the data cloud. It is a bell shaped curve which considers the reduction at both ends of the data set. In general, Minikin (1963), Goda (ex. Takahashi, 1994) and Allsop & Vicinanza (1996) methods are predicting the measured impulsive force on the vertical walls. However, PROVERBS (2001), Cuomo et al. (2010) and Blackmore & Hewson (1984) prediction methods are accurate for designing according to the results from small the scale tests for regular waves. .

PRESSURE DISTRIBUTION

Fig. 15~18 shows the comparison between the instantaneous pressure distribution for 5 impacts which creates the highest value force on the vertical wall and the predicted pressure profile for the envelope functions. Instantaneous pressure profile is determined from the pressure sensor results at the time of peak force calculated from Eq. 8 for each individual impact. Here results are shown for the 5 highest maximum values. There is a high scattering seen also for the location and value of peak pressures. Maximum peak pressures were observed between SWL and $0.5h_s$ above the SWL. Minikin, Blackmore & Hewson and PROVERBS methods (Fig15, 17 and 18) are fairly good assuming the upper boundary of the pressure profile. However all methods apparently do not predict the maximum peak pressures as found in the tests. There is a phase difference between the results of sensors at the upper corner part and the results of sensors at lower parts of the vertical wall. Due to the phase difference, the instantaneous pressure of upper corner shows negative values which appear just before impact rise. This phenomenon is described by Hattoria et al. (1994) as a result of an extremely high velocity jet shooting up the wall face.

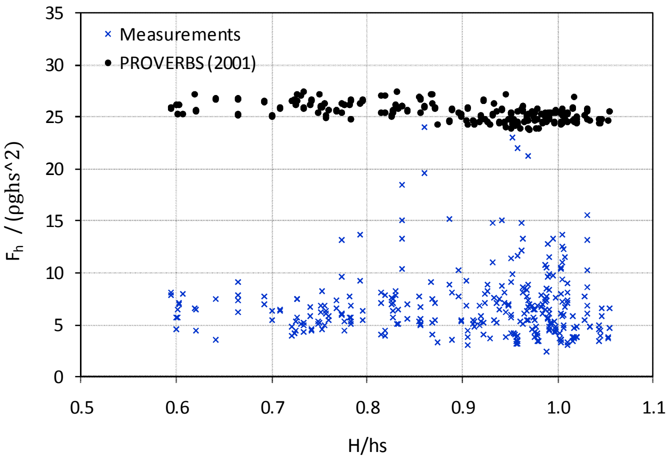

Figure 9. Comparison between the measured horizontal impact force on a vertical wall with the predicted horizontal force by PROVERBS formula. (Regular waves, T=2.2 s, h_s=0.135 m)

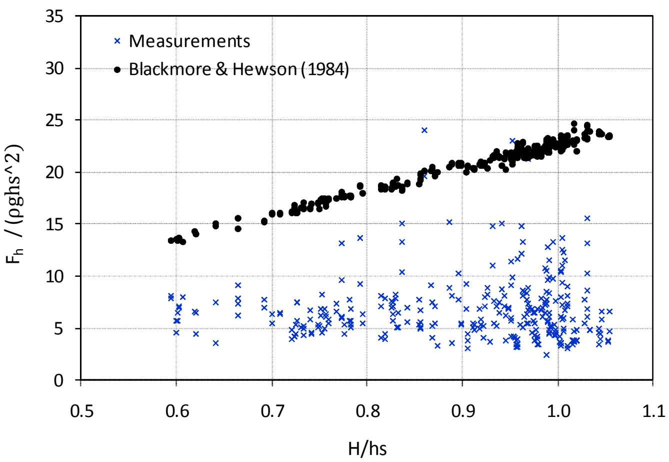

Figure 10. Comparison between the measured horizontal impact force on a vertical wall with the predicted horizontal force by Blackmore & Hewson formula. (Regular waves, T=2.2 s, h_s=0.135 m)

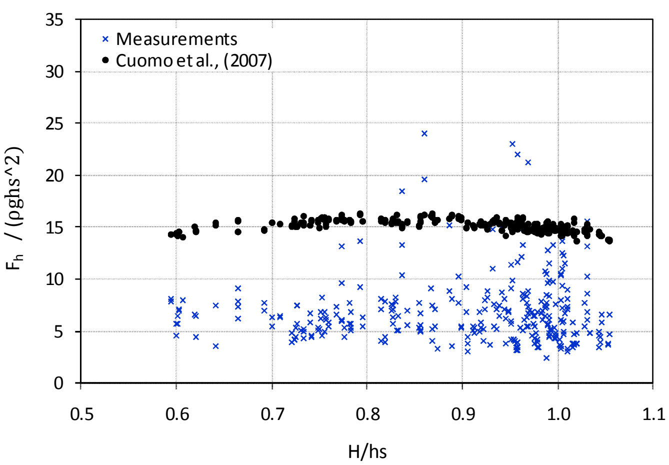

Figure 11. Comparison between the measured horizontal impact force on a vertical wall with the predicted horizontal force by Cuomo formula. (Regular waves, T=2.2 s, h_s=0.135 m)

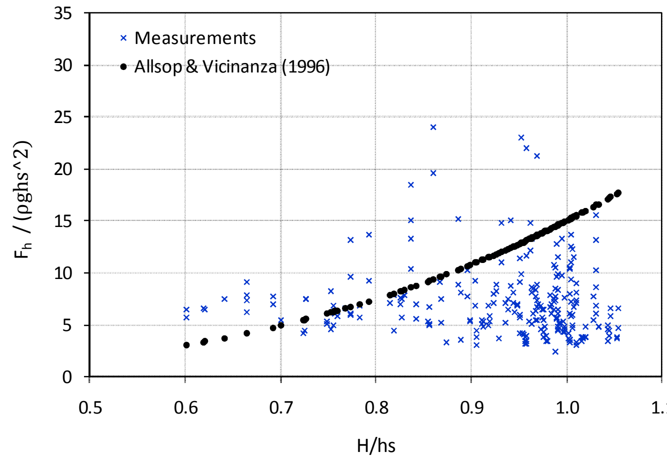

Figure 12. Comparison between the measured horizontal impact force on a vertical wall with the predicted horizontal force by Allsop & Vicinanza formula. (Regular waves, T=2.2 s, h_s=0.135 m)

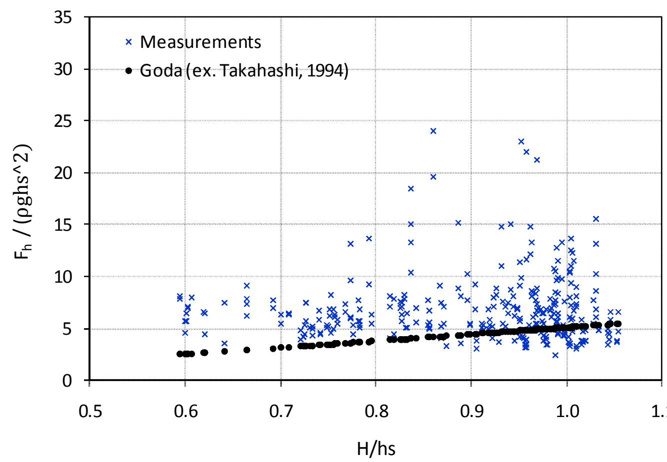

Figure 13. Comparison between the measured horizontal impact force on a vertical wall with the predicted horizontal force by Goda formula (ex. Takahashi) (Regular waves, T=2.2 s, h_s=0.135 m).

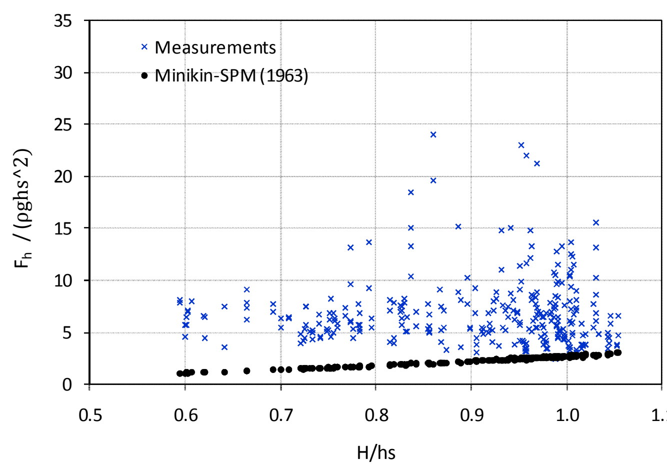

Figure 14. Comparison between the measured horizontal impact force on a vertical wall with the predicted horizontal force by Minikin formula (SPM version) (Regular waves, T=2.2 s, h_s=0.135 m).

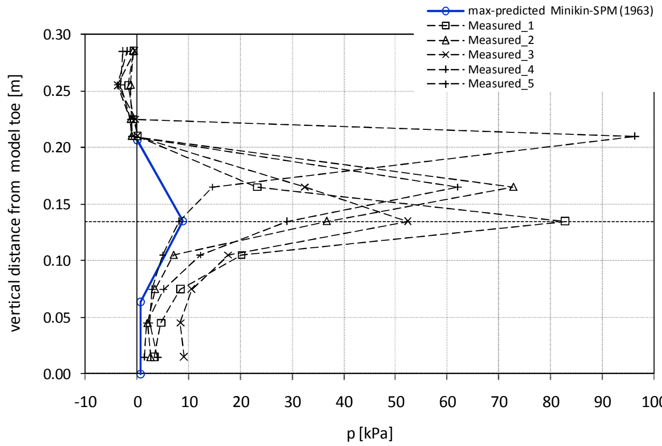

Figure 15. Comparison between the measured vertical pressure profile of 5 waves creating the highest impact force with the highest predicted pressure profile using the Minikin method. (Regular waves, T=2.2 s, h_s=0.135 m)

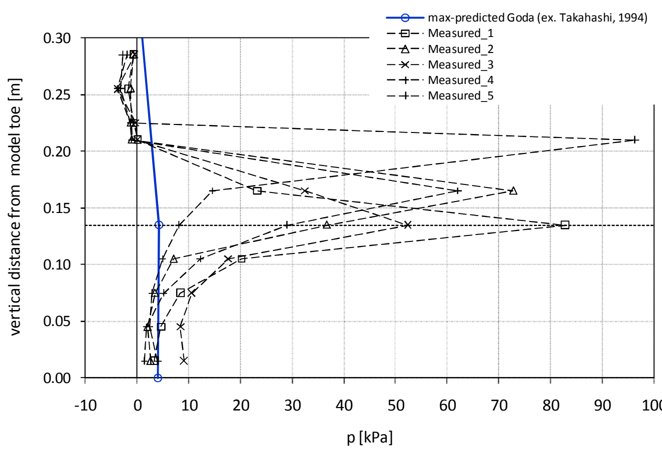

Figure 16. Comparison between the measured vertical pressure profile of 5 waves creating the highest impact force with the highest predicted pressure profile using the Goda (extended) method. (Regular waves, T=2.2 s, h_s=0.135 m)

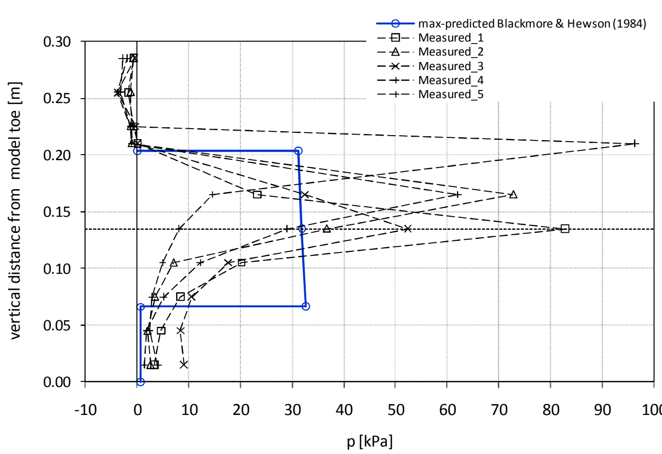

Figure 17. Comparison between the measured vertical pressure profile of 5 waves creating the highest impact force with the highest predicted pressure profile using the Blackmore & Hewson method. (Regular waves, T=2.2 s, h_s=0.135 m)

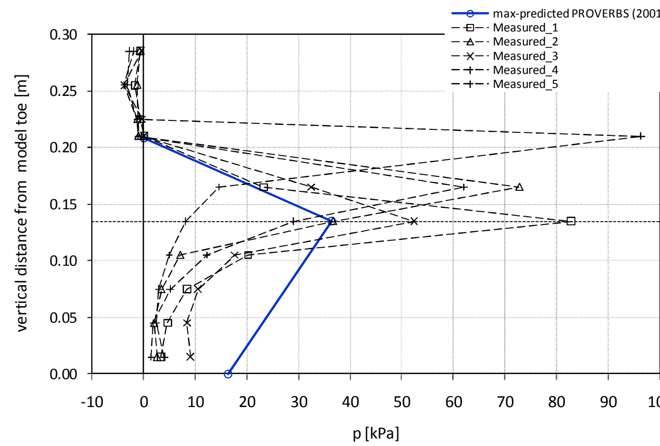

Figure 18. Comparison between the measured vertical pressure profile of 5 waves creating the highest impact force with the highest predicted pressure profile using the PROVERBS method. (Regular waves, T=2.2 s, h_s=0.135 m)

COMPARISION BETWEEN TEST RESULTS OF MODEL-A AND MODEL-B

Fig. 19 and Fig. 20 show the comparison between the measured horizontal force and the overturning moment both on a simple vertical wall (Model-B) and a vertical wall with cantilever slab (Model-A). Force and overturning moments are shown on axis of wave height (H) normalized by water depth h_s. A significant increases observed on the horizontal force of Model-A compared to Horizontal force on Model-B (Fig. 19). This is mainly caused by the effect of a second impact occurring at the corner of the overhanging part fixed to the vertical wall. This secondary impact is the result of jets climbing on the vertical wall and slamming on the horizontal part. Increase of the horizontal force is more significant in the zone of breaking wave with small air trapping ($0.6 < Hh_s < 0.9$). In the zone of breaking with large air trapping ($0.9 < Hh_s < 1.1$), waves are curving more which results in weak vertical jets and weak pressure on the overhanging part. The effect of pressure on the overhanging part due to the secondary impact is more important for the overturning moment (Fig. 20).

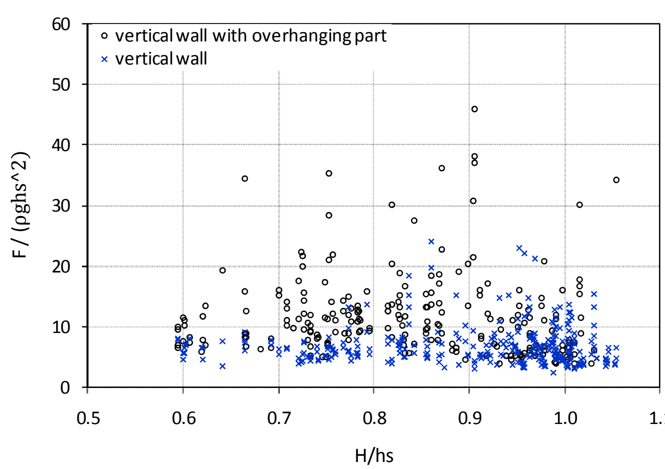

Figure 19. Comparison between the measured horizontal force F_h on the simple vertical wall (Model-B) and the vertical wall with cantilever slab (Model-A) (Regular waves, T=2.2 s, h_s=0.135 m)

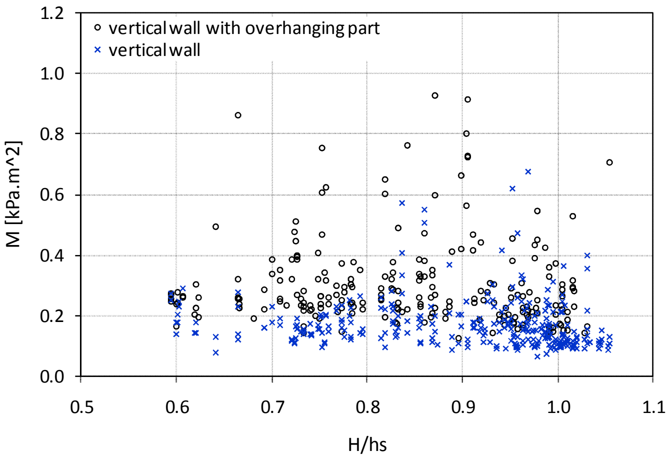

Figure 20. Comparison between the measured overturning moment M on the simple vertical wall (Model-B) and the vertical wall with cantilever slab (Model-A) (Regular waves, T=2.2 s, h_s=0.135 m)

CONCLUSIONS

A simple vertical wall (Model-B) and a vertical wall with cantilevering slab (Model-A) are tested in a small scale test set-up (at scale 1:20) using regular waves for four different values of water depth and wave period. All the events have been recorded by a high speed camera with 250 frames per second. Pressures on the models have been measured by 10 pressure sensors using 20 kHz sampling frequency. On model-A, the largest peak pressures were recorded at the SWL ($82 * \rho g h_s$) on the vertical part and at the corner of the horizontal part ($90 * \rho g h_s$). Force and pressure measurements on the simple vertical wall (Model-B) were used to evaluate the existing prediction formulas. Prediction formulas of Minikin (1963), Goda (ex. Takahashi, 1994) and Allsop & Vicinanza (1996) under estimate the impulsive force on the vertical walls. Prediction formulas of PROVERBS (2001), Cuomo et al. (2010) and Blackmore & Hewson (1984) are overestimating the force.

A significant effect of the overhanging part is observed on the total horizontal force and overturning moment of Model-A. This is due to a secondary impact occurring on the overhanging part by a jet climbing on the vertical part.

REFERENCES

Allsop, N.W.H.; McKenna, J.E.; Vicinanza, D.; and Whittaker, T.J.T. (1996), New design formulae for wave loadings on vertical breakwaters and seawalls, Proc 25th Int. Conf. Coastal Engineering, ASCE, New York (1996), pp. 2508–2521.

Allsop, N.W.H.; Vicinanza, D.; Calabrese, M.; Centurioni, L., (1996c), "Breaking Wave Impact Loads on Vertical Faces", ISOPE-International Offshore and Polar Engineering-Conference, pp-185, Los Angeles, California

Allsop, N.W.H.; Vicinanza, D.; McKenna, J.E., (1996), "Wave forces on vertical and composite breakwaters", Strategic Research Report SR 443, HR Wallingford, Wallingford (1996), pp. 1–94 March 1996

Blackmore, P.A.; Hewson, P.J., (1984), "Experiments on full-scale wave impact pressures", *Coastal Engineering* Volume:08 Issues:4, pp:331-346

Bullock, G; Obhrai, C.; Müller, G.; Wolters, G.; Peregrine, H.; Bredmose, H., (2004), "Characteristics and design implications of breaking wave impacts" -Coastal Engineering Conference, pp: 3966

Cuomo G.; Tirindelli M.; and William Allsop W., 2007, '*Wave-in-deck loads on exposed jetties*', Coastal Engineering Volume 54, Issues-9, 2007, pp: 657-679

Cuomo, G; Allsop, W; Bruce, T; Pearson, J, (2009), Breaking wave loads at vertical seawalls and breakwaters, *Coastal Engineering, In Press,* Corrected Proof, Available online 20 January 2010

Cuomo, G; Allsop, W; Bruce, T; Pearson, J, (2010), Breaking wave loads at vertical seawalls and breakwaters, Coastal Engineering, In Press, Corrected Proof, Available online 20 January 2010

Goda, Y. (1974), "New wave pressure formulae for composite breakwater, Proc. of 14th Int. Conf. Coastal Eng., Copenhagen, Denmark, ASCE, New York (1974), pp. 1702–1720.

Goda, Y. (2000), 'Random seas and design of maritime structures" (2nd Edition), *Advanced Series on Ocean Engineering* vol. 15, World Scientific (2000) 443 pp

Hattori, M.; Arami, A.; Yui, T., (1994), "Wave impact pressure on vertical walls under breaking waves of various types", Coastal-Engineering, Volume:22 Issues:1-2-1994-pp-79-114

McConnell, K.J; Allsop, N.W.H; Cuomo, G; and. Cruickshank, I.C, 2003, '*New guidance for wave forces on jetties in exposed locations*', Paper to Conf. COPEDEC VI, Colombo, Sri Lanka pp: 20

Okamura, M., (1993), '*Impulsive pressure due to wave impact on an inclined plane wall*', Fluid Dynamics Research, volume 12, issue 4, pp. 215-228

Oumeraci, H. (1994), "Review and analysis of vertical breakwater failures lessons learned Special Issue on Vertical Breakwaters", Coastal Eng. 22 (1994), pp. 3–29.

Oumeraci, H; Kortenhaus, A; Allsop, W; de Groot, M; Crouch, R; Vrijling, H; Voortman, H, (2001). "*Probabilistic Design Tools for Vertical Breakwaters*", Balkema Publishers, New York.

Shore Protection Manual. 1984. 4th ed., 2 Vol U.S. Army Engineer Waterways Experiment Station, U.S. Government Printing Office, Washington, DC

Shore Protection Manual. 1984. 4th ed., 2 Vol U.S. Army Engineer Waterways Experiment Station, U.S. Government Printing Office, Washington, DC

Takahashi, S., (1996), "Design of vertical breakwaters", Port and Harbour Research Institute, Ministry of Transport, Reference documenr # 34.

Verhaeghe, H.; Cherlet, J.; Boone, C.; Troch, P.; De Rouck, J.; Awouters, M.; Ockier, M.; Devos, G., 2006, '*Prototype monitoring of wave loads on concrete structure in intertidal zone*', Proceedings of the First International Conference on the Application of Physical Modelling to Port and Coastal Protection COASTLAB06. pp. 117-125